HHS Public Access

Author manuscript

J Microsc. Author manuscript; available in PMC 2017 July 01.

Published in final edited form as:

J Microsc. 2016 July ; 263(1): 113–117. doi:10.1111/jmi.12385.

Micro-CT scouting for transmission electron microscopy of human tissue specimens

A. G. MORALES[*], **E. S. STEMPINSKI**[*], **X. XIAO**[†], **A. PATEL**[*], **A. PANNA**[*], **K. N. OLIVIER**[*], **P. J. MCSHANE**[*], **C. ROBINSON**[*], **A. J. GEORGE**[*], **D. R. DONAHUE**[‡], **P. CHEN**[*], and **H. WEN**[*]

[*]National Heart Lung and Blood Institute, National Institutes of Health, Bethesda, Maryland, U.S.A

[†]Advanced Proton Source, Argonne National Laboratory, Lemont, Illinois, U.S.A

[‡]National Institute of Neurological Disorders and Stroke, National Institutes of Health, Bethesda, Maryland, U.S.A

Summary

Transmission electron microscopy (TEM) provides sub-nanometer-scale details in volumetric samples. Samples such as pathology tissue specimens are often stained with a metal element to enhance contrast, which makes them opaque to optical microscopes. As a result, it can be a lengthy procedure to find the region of interest inside a sample through sectioning. We describe micro-CT scouting for TEM that allows non-invasive identification of regions of interest within a block sample to guide the sectioning step. In a tissue pathology study, a bench-top micro-CT scanner with 10 μm resolution was used to determine the location of patches of the mucous membrane in osmium-stained human nasal scraping samples. Once the regions of interest were located, the sample block was sectioned to expose that location, followed by ultra-thin sectioning and TEM to inspect the internal structure of the cilia of the membrane epithelial cells with nanometer resolution. This method substantially reduced the time and labor of the search process from typically 20 sections for light microscopy (LM) to 3 sections with no added sample preparation.

Keywords

micro-CT scouting; transmission electron microscopy; three-dimensional visualization; bench-top micro-CT scanner

Introduction

Micro-CT is non-invasive and can provide 3D visualization with minimal sample preparation. It has many uses in the fields of material science and pre-clinical studies of animal models, in-vivo and ex-vivo, as well as human tissue specimen studies (Hildebrand *et al.*, 1999, Laib *et al.*, 2001, Momose *et al.*, 1996, Stock, 1999, Stock *et al.*, 2003). When micro-CT images are correlated with light and electron microscopy, they provide a valuable

Correspondence to: Han Wen, National Heart Lung and Blood Institute, National Institutes of Health, Bethesda, 20892 MD, U.S.A. Tel: +1-301-496-2694; fax: +1-301-402-2389; han.wen@nih.gov.

three-dimensional global context for detailed structures (Handschuh *et al.*, 2013, Lareida *et al.*, 2009, Pai *et al.*, 2012, Sengle *et al.*, 2013, Stalder *et al.*, 2014). Although previous studies have demonstrated beautiful correlations between light microscopy, electron microscopy and micro-CT images in select samples, to our knowledge, this is the first study to show how standard bench-top micro-CT can substantially speed up the workflow and reduce the labor of TEM for a large number samples. For samples up to 15 millimeters in size, current commercial bench-top micro-CT scanners can cover the entire sample at pixel sizes of several microns, and true resolution of about 10 μm in standard scans (Pai et al., 2012). This resolution was sufficient to non-invasively locate the region of interest (ROI) in osmium-stained human nasal scraping samples for the subsequent TEM study. Due to osmium staining, the samples are opaque to visible light (Fig. 1). The micro-CT volume data indicated which samples, or parts of samples, contained a mucous membrane, and which contained just blood. The information was used to guide the sectioning of the epoxy blocks and indicate ROIs in the sections for subsequent LM and TEM of the epithelial cilia on the nasal mucous membrane in these patients.

Before the use of micro-CT, the traditional scouting method for epoxy blocks was sectioning, followed by staining and light microscopy to determine whether patches of the mucous membrane were found, and whether an epithelial surface, likely to contain cilia, had been exposed. A typical search involves 20 such cycles per sample. The labor and time needed to do so in hundreds of samples are staggering. To solve this challenge we used a bench-top micro-CT scanner to non-invasively locate regions of interest in 3D, which guides the sectioning process and reduces the search to two or three light-microscopy sections per sample. In addition to the bench-top micro-CT scans, sub-micron resolution CT images were acquired at a synchrotron beamline. The synchrotron beam had sufficient brightness to differentiate individual cells in a short scan. The synchrotron images helped us understand and interpret the lower resolution bench-top micro-CT images.

Materials and methods

Sample collection and preparation

Under an institutional review board (IRB) approved clinical protocol on the natural history of bronchiectasis, nasal scraping samples were collected from bronchiectasis patients with chronic and recurring respiratory tract infections to study the changes of the molecular structures in the cilia of the epithelial cells of the mucous membrane (Olin *et al.*, 2011). Curettes with nasal tissue were immediately fixed in 2% glutaraldehyde, 2% paraformaldehyde, and 0.5% tannic acid in sodium phosphate buffer, pH 7.2. The tissue was removed from the curette, washed in sodium phosphate buffer, post-fixed in 1% osmium tetroxide in phosphate buffer, *en bloc* stained with 1% uranyl acetate, dehydrated in an ethanol series and propylene oxide, and embedded in EMbed 812 resin (Electron Microscopy Sciences, Hatfield PA) as shown in Fig. 1. Sections were cut on an Ultracut UCT ultramicrotome (Leica Microsystems, Buffalo Grove IL). The epoxy resin blocks were formed in molds which were matched to the chucks of the ultramicrotome. In the ultramicrotome, the blocks were held in the chucks such that the sections were perpendicular to the axis of the blocks, or the Z axis.

Micro-CT scan

We used a Bruker Skyscan 1172 bench-top micro-CT for the scouting scans. The epoxy block samples were mounted vertically along the rotation axis and centered on the osmium stained tip of the block. The scans covered a 180° rotation angle in 450 or 900 projections. X-ray tube settings were 29 to 59 kV and 0.17 mA. The total scan time was between 2 and 3 hours. The vendor NRecon software was used to reconstruct 3D volumes at 1.09 μm isotropic voxel size. The actual resolution was limited by the spot size of the x-ray tube to about 10 μm. Since the axis of the epoxy blocks were aligned with the CT rotation axis, the Z axis distance from the top of the specimen to an interior location in the micro-CT volume data corresponded to the sectioning depth on the ultramicrotome, accurate to within the CT resolution of 10 μm.

Additional high-resolution micro-CT scans were carried out at the 2-BM-A beamline of the Advanced Proton Source (APS) of the Argonne National Laboratory. The raw projection images had 0.65 μm pixel size over a 1.6 mm × 1.3 mm field of view. Over the 180° rotation 2000 projections were acquired at 100 ms exposure per projection and a rotation speed of 0.75 deg/s. The total scan time was 4 minutes. Photon energies were set to 30 keV. Custom software by APS was used to reconstruct the 3D volumes at 0.65 μm isotropic voxel size.

Light microscopy and transmission electron microscopy

To find the ROI by the standard sectioning procedure, the sample was sectioned at 0.5 μm in an ultramicrotome. Every 100th section was stained with toluidine blue and inspected under a Leica DMB-4000 light microscope equipped with a digital camera (Leica Microsystems, Buffalo Grove IL) until patches of the mucous membrane were found, and there were indications of cilia on the epithelial surface. Then sections 60 nm in thickness were stained with uranyl acetate and lead citrate prior to imaging with a JEM1400 electron microscope (JEOL USA, Peabody MA) with an AMT XR-111 digital camera (Advanced Microscopy Techniques Corporation, Woburn MA).

In the procedure assisted by micro-CT scouting, locations containing epithelia surfaces of the mucous membrane were identified in the CT volume. The sample was then sectioned to the target location at 0.5 μm steps based on the known depth from the surface. At this point 2 to 3 sections were examined by LM to confirm the match to the CT image. Once the location was confirmed, if LM showed the presence of ciliated epithelial cells, then 60 nm thick sections were cut and TEM performed. Otherwise the process was repeated on the next target location in the sample. It is worth noting that the LM and TEM sections were adjacent and a few microns apart, such that they contained similar but not identical tissue structures.

Results

An example of micro-CT scouting for TEM is illustrated in Fig. 2. The micro-CT data of an epoxy block is rendered in 3D and shows the osmium stained volume of the nasal scraping sample near the tip of the block (Fig. 2A). The 3D volume consists of a stack of 2074 transverse slices. Osmium stained areas appear bright in the micro-CT slices. A slice taken 1.24 mm from the surface (Fig. 2B) has an osmium-stained area of relatively uniform

brightness, smooth borders and organized texture, which is recognized as potential regions of nasal epithelial tissue containing ciliated cells. Fig. 2C is a magnified view of a slice from the synchrotron micro-CT data which matches the bench-top micro-CT slice in Fig. 2B. The sample was sectioned at 0.5 μm steps to this level and light microscopy confirms the presence of epithelial cells at this location (Fig. 2D). An area containing epithelial cells (outlined in the LM image) was identified, and in the subsequent 60 nm section, the corresponding area was inspected by TEM (Fig. 2E) and revealed ciliated cells. Further magnification of a sub-region that contains perpendicular cilia revealed the 9 outer doublets and 2 central singlets of microtubules in each cilium (Fig. 2F). When compared with the bench-top micro-CT scanner, the synchrotron image has higher resolution. It shows structures in the tissue that can be identified to individual cells in the light microscopy image in Fig. 2C. The brighter areas in the synchrotron micro-CT image match the darker stained areas in the LM image. As described in the Materials and Methods section, the TEM protocol dictates that the LM and TEM sections are separated by a few microns. Thus, the corresponding images were similar but not identically matched.

In the second example we illustrate how micro-CT was used to rule out an invalid sample. In this sample the bench-top micro-CT showed diffused osmium staining of unorganized grainy texture throughout the stained volume (Fig. 3A). The corresponding synchrotron micro-CT slice revealed the texture as discrete dots of osmium concentration (Fig. 3B). Both light microscopy (Fig. 3C) and TEM (Fig. 3D) revealed that these were individual red blood cells, which was the predominant content of the sample. It was concluded that this nasal scraping sample did not contain mucous membrane tissue.

Discussion

In a prior study of 60 osmium-stained mouse heart specimens, the bench-top micro-CT scanner at 10 μm resolution demonstrated the ability to visualize coronary artery wall structures down to the secondary, and sometimes tertiary branches, that matched histological sections of the specimens (Pai et al., 2012). In this study the bench-top scanner was sufficient to identify tissues within epoxy block samples as targets for light microscopy and TEM. Micro-CT provided a useful vantage point for imaging a large field of view which was sufficient to cover the epoxy blocks. Although the resolution of the bench-top system could not resolve individual cells, by correlating the images with light microscopy and synchrotron CT images in a few samples, we learned to recognize the characteristics of mucous membrane tissue in the data from the bench-top scanner. Therefore, this “learn and scout” method benefits the electron microscopy of repetitive tissue specimens where the samples are relatively large and the search process is lengthy by standard sectioning.

Our TEM study needed to locate transverse cross sections of the epithelial cilia of the nasal mucosa to see the microtubules within the cilia. By micro-CT scouting we were able to accurately locate the sections that contained the mucous membrane and identify ROIs within these sections, as verified by LM. The cilia were not visible in micro-CT and marginally visible in LM. The regions of interest from micro-CT all contained cilia, but only one in three contained cilia that were perpendicular to the plane of the sections and offered the right cross-section images under TEM.

Although the high-resolution synchrotron scans in our study are not expected to be a routine scouting step, they helped us to better understand the images obtained with the bench-top micro-CT scanner, and to better correlate them to the light microscopy images. They also provided an incentive to develop laboratory micro-CT scanners that can scan large samples at higher resolution.

When using a laboratory CT scanner as a routine scouting step for TEM studies, the key consideration is the balance between resolution and scan time. A major limitation for laboratory systems seems to be the basic vacuum tube design of the x-ray source. It sets a relationship between the focal spot size and the attainable output flux, which is limited by the heat load density on the anode surface. Specifically, the bench-top scanner we used could theoretically provide near 5 μm resolution at a low flux output, which would have lengthened our scans by a factor of 3, without considering focal spot stability concerns; Larger laboratory nano-CT systems (about 2 meters footprint and 2 tons weight) with scalable resolutions feature sub-micron focal spot sizes (for example, systems from Bruker, GE Nanotom and Xradia/Zeiss, among others), although the scan time scales up quickly with better resolution, again, due to the fixed relationship between focal spot size and photon output. Zone-plate (Fresnel lens) based nano-CT systems are less limited by the tube focal spot size and can achieve better than 100 nm resolution, but with a substantial reduction of efficiency, due to the efficiency of zone plates and reduced fields of view because of the size of the zone plates. Ultimately, future breakthroughs in x-ray source technology may completely change the situation and enable laboratory systems to reach 1 μm or better resolution in a reasonable scan time for scouting applications.

Another consideration, which relates to the balance between sample size and resolution, is the X-ray photon energy needed to penetrate the sample. Thicker samples will require higher kV settings for the micro-CT scanner, which may lead to a higher power setting on the X-ray tube and as a result, larger focal spot size yielding lower resolution.

Both resolution and scan time are also influenced by the efficiency of the detector. Similar to the direct-detection cameras in electron microscopes, the latest X-ray photon-counting detectors and image intensifier technology may soon allow bench-top micro-CT systems to reach ideal levels of detector efficiency.

Acknowledgments

We are grateful to Patricia Connelly of the NHLBI EM Core for her assistance with electron microscopy. We are grateful to Douglas Morris of the NIH Mouse Imaging Facility for his assistance with micro-CT. This research used resources of the Advanced Photon Source, a U.S. Department of Energy (DOE) Office of Science User Facility operated for the DOE Office of Science by Argonne National Laboratory under Contract No. DE-AC02-06CH11357.

References

Handschuh S, Baeumler N, Schwaha T, Ruthensteiner B. A correlative approach for combining microCT, light and transmission electron microscopy in a single 3D scenario. Frontiers in Zoology. 2013; 10

Hildebrand T, Laib A, Müller R, Dequeker J, Rüegsegger P. Direct Three-Dimensional Morphometric Analysis of Human Cancellous Bone: Microstructural Data from Spine, Femur, Iliac Crest, and Calcaneus. Journal of Bone and Mineral Research. 1999; 14:1167–1174. [PubMed: 10404017]

Laib A, Kumer JL, Majumdar S, Lane NE. The Temporal Changes of Trabecular Architecture in Ovariectomized Rats Assessed by MicroCT. Osteoporos Int. 2001; 12:936–941. [PubMed: 11804020]

Lareida A, Beckmann F, Schrott-Fischer A, Glueckert R, Freysinger W, Müller B. High-resolution X-ray tomography of the human inner ear: synchrotron radiation-based study of nerve fibre bundles, membranes and ganglion cells. Journal of Microscopy. 2009; 234:95–102. [PubMed: 19335460]

Momose A, Takeda T, Itai Y, Hirano K. Phase-contrast X-ray computed tomography for observing biological soft tissues. Nat Med. 1996; 2:473–475. [PubMed: 8597962]

Olin JT, Burns K, Carson JL, Metjian H, Atkinson JJ, Davis SD, Dell SD, Ferkol TW, Milla CE, Olivier KN, Rosenfeld M, Baker B, Leigh MW, Knowles MR, Sagel SD. Diagnostic yield of nasal scrape biopsies in primary ciliary dyskinesia: a multicenter experience. Pediatric pulmonology. 2011; 46:483–488. [PubMed: 21284095]

Pai VM, Kozlowski M, Donahue D, Miller E, Xiao X, Chen MY, Yu ZX, Connelly P, Jeffries K, Wen H. Coronary artery wall imaging in mice using osmium tetroxide and micro-computed tomography (micro-CT). Journal of Anatomy. 2012; 220:514–524. [PubMed: 22360411]

Sengle G, Tufa SF, Sakai LY, Zulliger MA, Keene DR. A correlative method for imaging identical regions of samples by micro-CT, light microscopy, and electron microscopy: imaging adipose tissue in a model system. The journal of histochemistry and cytochemistry: official journal of the Histochemistry Society. 2013; 61:263–271. [PubMed: 23264636]

Stalder AK, Ilgenstein B, Chicherova N, Deyhle H, Beckmann F, Müller B, Hieber SE. Combined use of micro computed tomography and histology to evaluate the regenerative capacity of bone grafting materials. International Journal of Materials Research. 2014; 105:679–691.

Stock SR. X-ray microtomography of materials. International Materials Reviews. 1999; 44:141–164.

Stock SR, Ignatiev K, Dahl T, Barss J, Fezzaa K, Veis A, Lee WK, De Carlo F. Multiple microscopy modalities applied to a sea urchin tooth fragment. Journal of Synchrotron Radiation. 2003; 10:393–397. [PubMed: 12944629]

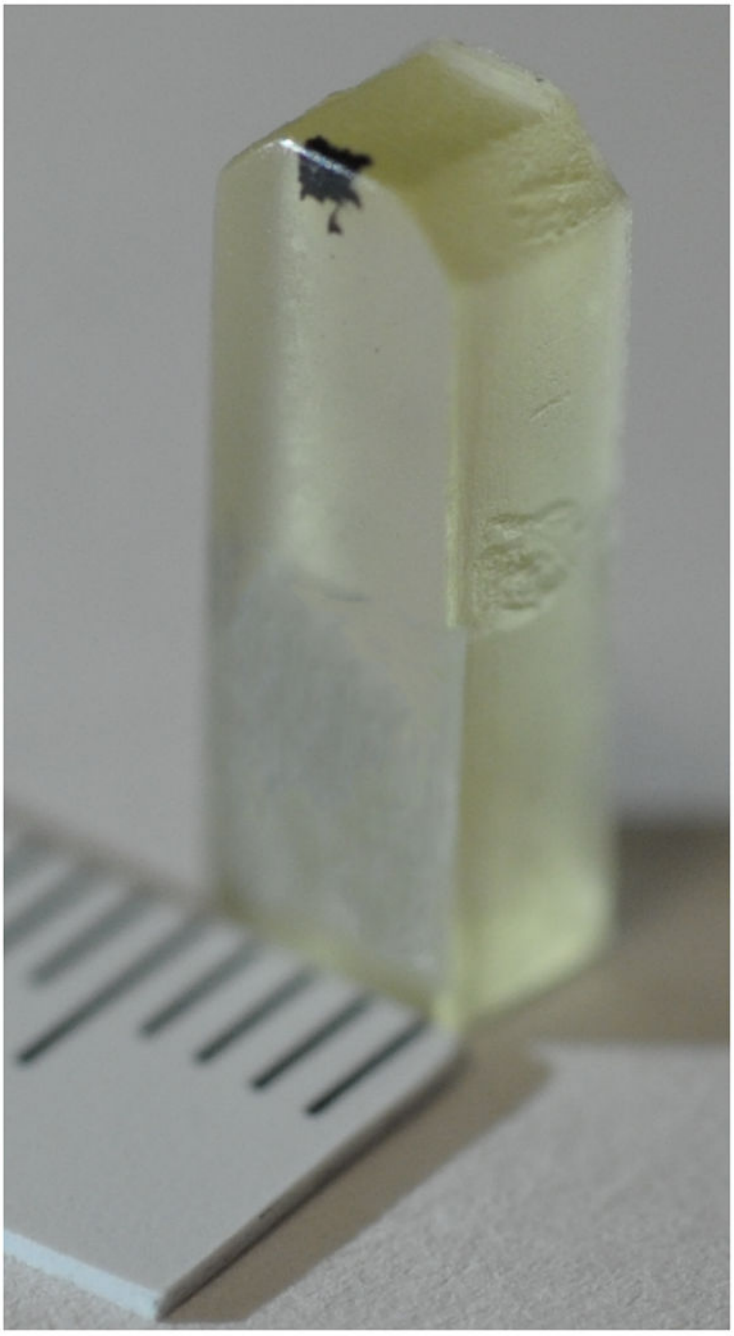

Figure 1.
An epoxy block for TEM. The osmium-stained human nasal scraping sample appears as a black patch near the top edge of the block. Scale is in mm.

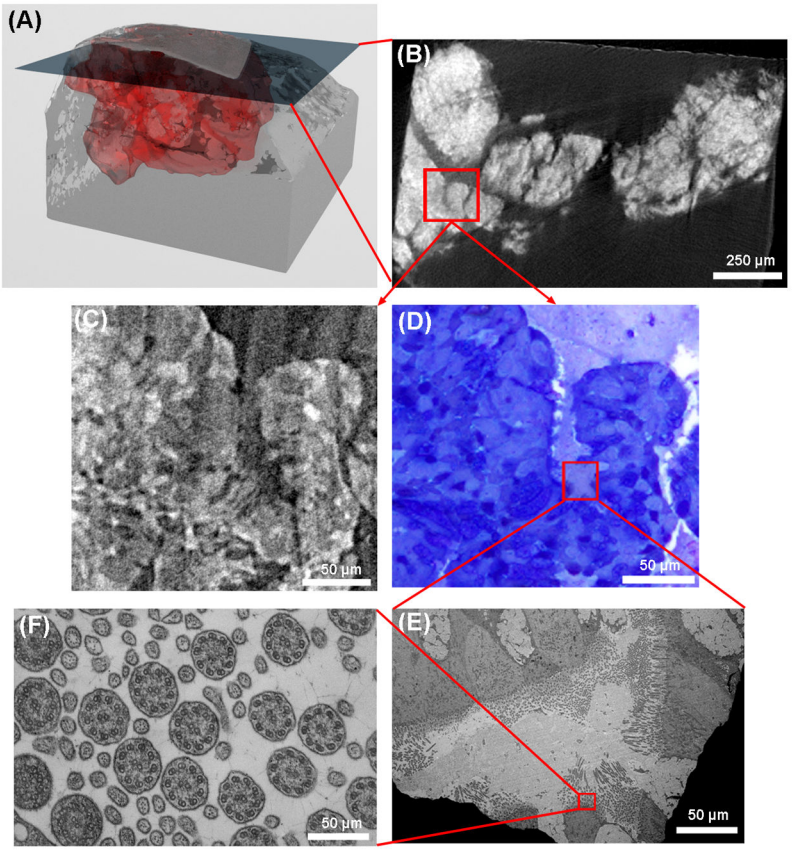

Figure 2.

An illustration of micro-CT guided TEM of a nasal scraping sample. (A) The bench-top micro-CT data is rendered in 3D, with the red region representing the osmium stained specimen. A cross-section slice through the 3D volume is shown in (B) where brighter areas represent higher x-ray attenuation due to the presence of osmium. An area outlined by the red square has relatively uniform brightness with organized textures and relatively smooth borders, which is recognized as mucous membrane tissue. A magnified view of the outlined area from the synchrotron CT data is shown in (C). The sample was sectioned to the location of this slice, stained and examined under light microscopy. The LM image of the same area, shown in (D), confirms the presence of epithelial cells of the mucous membrane. There is visual resemblance between the CT image in (C) and the LM image in (D). In a subsequent 60 nm section, the area next to the red outlined region in (D) is magnified in the TEM image (E). Cilia of various orientations are visible. A sub-region outlined in the red square is further magnified with TEM in (F), showing cross-sections of the cilia and the microtubule arrangement in them. The sections for LM and TEM were necessarily adjacent but different sections, leading to a slight mismatch between the LM and TEM images.

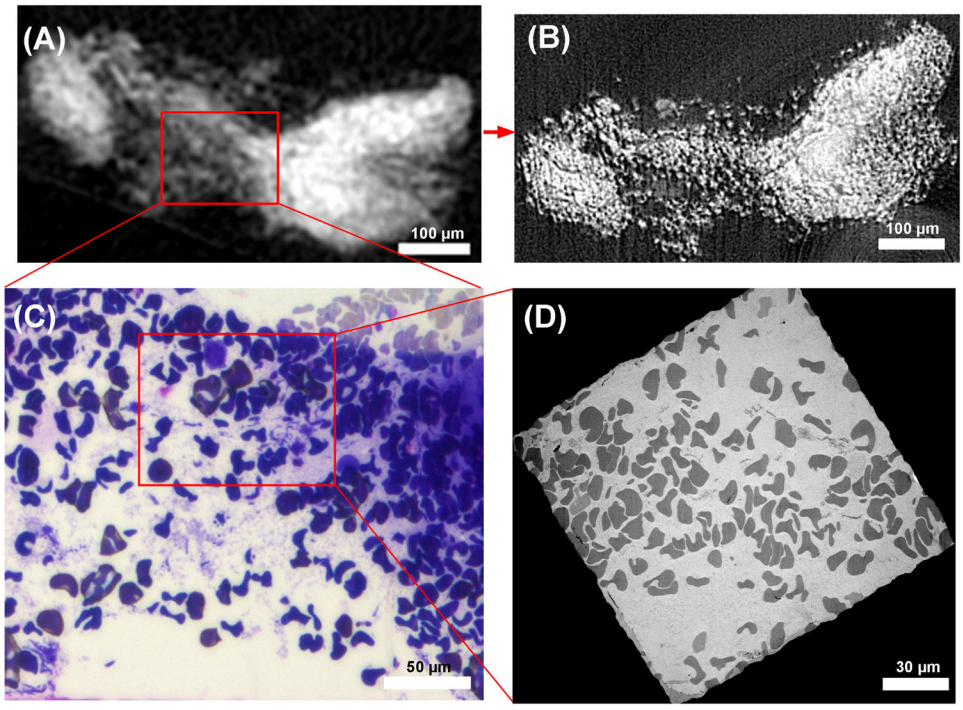

Figure 3.

Imaging sequence of a specimen which was determined to be invalid for the clinical study. (A) A slice through the bench-top micro-CT data shows an unorganized grainy texture. (B) The same slice from the higher resolution synchrotron CT data reveals that the unorganized grainy texture is discrete dots of osmium concentration. (C) The sample was sectioned to the location of the slice, and light microscopy image resolved the dots as red blood cells. (D) Transmission electron microscopy image of a section at the same location confirms the finding. The example illustrates how the bench-top scanner at 10 μm resolution provided sufficient information to exclude invalid samples. The higher resolution synchrotron CT helped to better understand the images from the bench-top scanners. The LM and TEM sections were necessarily separated by a few microns and the details of the LM and TEM images differ at the level of individual red blood cells.